Wind tunnel tests of wings at Reynolds numbers below 70 000

E. V. Laitone

Abstract Rectangular planform wings were tested at Reynolds numbers as low as 20 000 in a low turbulence wind tunnel. The lift and drag measurements on a NACA 0012 profile were compared with those for thin flat and cambered plates. For all Reynolds numbers below 70 000 the best profile was a thin plate with a 5% circular arc camber. At all turbulence levels this profile produced the greatest lift-drag ratio, and had the highest lift coefficient at all angles of attack. The 5% camber and all of the thin plates tested were relatively insensitive to either a variation in the Reynolds number, or an increase in the wind tunnel turbulence level, whereas the NACA 0012 was very seriously affected by either, at Reynolds numbers below 50 000.

List of symbols

A	aspect ratio = (span/chord)
c	wing chord = 0.031 m
C_D	$D/(S\rho V_\infty^2/2)$ = drag force coefficient parallel to wind tunnel axis
C_L	$L/(S\rho V_\infty^2/2)$ = lift force coefficient perpendicular to wind tunnel axis
Re	Reynolds number = $V_\infty c\rho/\mu$
S	wing planform area (m^2)
V_∞	free-stream velocity ahead of wing (m/s)
α	angle of attack of wing chord line relative to wind tunnel axis
$\Delta\alpha$	angle of attack from zero lift

Subscripts

o	value at $C_L = 0$
e	value corrected for wing planform and Re effects

1
Introduction

The aerodynamic forces on wings at low Reynolds numbers has become of interest again because of the planned use of small remotely piloted vehicles at very high altitudes. Schmitz (1941) investigated the aerodynamic forces on rectangular planform wings with an aspect ratio of five at Reynolds numbers as low as 20 000 because this data would be useful for analyzing the flight of birds and model aircraft. This data would also

E. V. Laitone
Department of Mechanical Engineering
University of California
Berkeley, CA 94702, USA

be useful for understanding limitations on small models in wind tunnel tests. It could be very helpful in explaining any unexpectedly low power outputs from wind tunnel tests of wind turbines whose model rotor blades generally operate at low Reynold numbers. However, Schmitz (1941) failed to obtain reliable data at a Reynolds number of 20 000 because his force balance was sensitive to only ± 0.10 g. More recently Mueller (1982, 1987) measured the lift forces on wings at Reynolds numbers as low as 40 000, but was unable to obtain reliable drag force data at this low Reynolds number because his two-component strain gauge balance was sensitive to only ± 1 g. Similarly, Marchman (1987) was unable to obtain reliable drag force data to complement his lift force data at low Reynolds numbers.

Since the main objective of the present tests was to measure the lift and drag forces on finite aspect ratio wings at low Reynolds numbers, a very sensitive two-component beam balance was designed with a precision ball bearing universal joint connecting two orthogonal beam balance arms. This balance had a sensitivity of ± 0.01 g, which was ten times more sensitive than the force balance used by Schmitz. The balance oscillations at the higher angles of attack and velocities were successfully eliminated by increasing the viscosity of the oil in the damping dash pot for the balance lift arm. All of the data presented are for the wings which had a chord of 31 mm, and were hung vertically from the beam balance which was mounted on the top of the test section. The upper wing tip was connected to the balance by a 3 mm diameter rod soldered to the mid-chord of the upper wing tip which was eight chord lengths below the tunnel ceiling. The lower wing tip of the aspect ratio six wing was twelve chord lengths above the tunnel floor. The square test section had 0.813 m walls and a length of 3.66 m. The dynamic pressures were measured by a standard Betz manometer, accurate to 0.01 mm of water. The lowest test velocity was 10 m/s, corresponding to approximately 6 mm of water, and a tunnel empty turbulence level of 0.02%.

The turbulence in Schmitz's wind tunnel was much higher since he measured a turbulence factor of 1.06 by the relatively insensitive sphere test. Consequently, Schmitz missed the anomalous effects produced by decreasing turbulence levels on the aerodynamic lift produced by a 12% thick airfoil with a rounded leading edge.

2
Effect of Reynolds number on aerodynamic lift

The wind tunnel data obtained at $Re = 20\,700$ shown in Figs. 1 and 2 further supports the conclusions of Schmitz
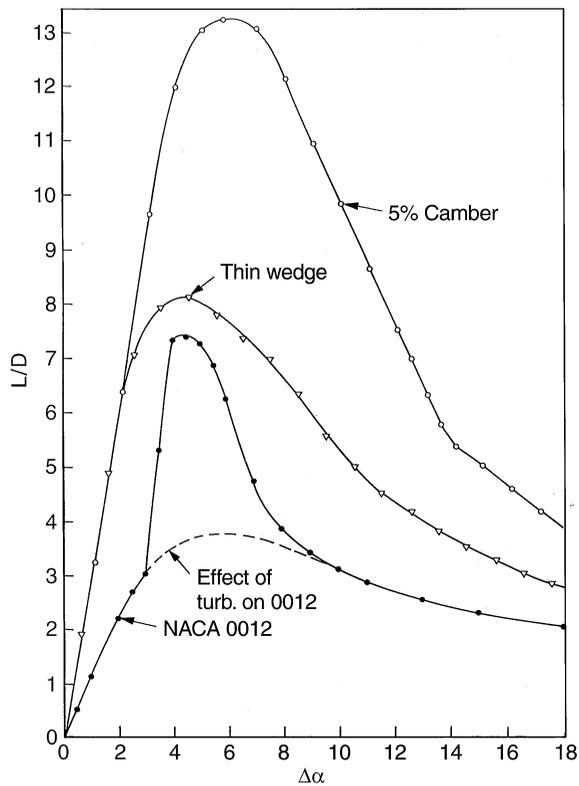
Fig. 1. Variation of the lift-drag ratio (L/D) with the angle of attack from zero lift ($\Delta\alpha$), for aspect ratio $A=6$, rectangular planform wings at $Re=20\,700$. Dashed line shows (L/D) loss from large increase in turbulence to that of the Schmitz (1941) wind tunnel (T.F.$=1.06$)

Fig. 2. Variation of lift coefficient (C_L) with the angle of attack from zero lift ($\Delta\alpha$) for aspect ratio $A=6$, rectangular planform wings at $Re=20\,700$. Dashed line shows loss of lift from large increase in turbulence to T.F.$=1.06$. NACA 0012 data now similar to wind tunnel tunnel data of Schmitz (1941)

(1941) that any airfoil's rounded leading edge, which is very important at high Re, becomes unsatisfactory at low Re. Figure 1 shows that the maximum lift-drag ratio of 13.3 is obtained by the 5% camber, which is a thin (1.3%) plate curved to a circular arc. Even the thin wedge, which has a 1% sharp leading edge and a blunt 4% trailing edge, has a lift-drag ratio of 8.15 which is 10% greater than the 7.4 for the NACA 0012. The thin wedge was used for all the data presented because it did not bend at high angles of attack at higher velocities. It was found that a sharp trailing edge was not necessary to develop lift at low Re, consequently the thin wedge produced the same lift as a 1% flat plate, however its lift-drag ratio was slightly lower because the drag increased with trailing edge thickness. While the 5% camber and the thin wedge lift forces were only slightly affected by increasing the wind tunnel turbulence level, Fig. 2 shows that at $Re=20\,700$ the NACA 0012 profile had a large decrease in lift when the turbulence level was greatly increased to correspond to that of the Schmitz (1941) wind tunnel tests (T.F.1.06). Fig. 1 shows that the NACA 0012 had its lift-drag ratio decreased 49% from 7.4 to 3.8 at this very high turbulence level. The dashed line data in Figs. 1 and 2 is similar to that given by Schmitz (1941) for the profile similar to the NACA 4412.

The unusual discontinuity in (C_L/α) at $\alpha=3°$ for the NACA 0012 did not occur at this highest turbulence level, as indicated

by the dashed line in Fig. 2. This (C_L/α) discontinuity was also decreased at $Re=42\,100$, as shown in Fig. 3, when ($C_L/\alpha)_o$ increased 49% from 0.041 to 0.061. As the Reynolds number increases the initial lift curve slope ($C_L/\alpha)_o$ also increases, while the (C_L/α) discontinuity at $C_L \approx 0.1$ decreases until it finally vanishes as the Reynolds number approaches 70 000 and the initial lift-curve slope ($C_L/\alpha)_o$ has increased to its highest value of 0.08. However at $Re=20\,700$ this (C_L/α) discontinuity for the NACA 0012 profile is not improved by a small increase in the wind tunnel turbulence level, as shown in Fig. 4 by the data for the NACA 0012 with a screen across the wind tunnel test section 1.2 m ahead of the wing. This increased the tunnel empty turbulence level from 0.02% to 0.10%, and increased the maximum lift coefficient at stall 30% from 0.455 to 0.59, and increased its lift-drag ratio 26% from 7.4 to 9.3. However the discontinuity in (C_L/α), and the initial slope ($C_L/\alpha)_o$ for the NACA 0012 were only slightly affected by the relatively small increase in the wind tunnel turbulence level by the screen, as shown in Fig. 4.

The discontinuity in (C_L/α) that is shown in Fig. 5 for the 5% camber at $\Delta\alpha \approx 14°$ still exists at $Re=20\,700$ if the wind tunnel turbulence level is increased from 0.02% to 0.10%. It is of interest to note that although C_L is increased by turbulence, C_D is also increased the same percent so that the lift-drag ratio remains identical to that given in Fig. 1 for the 5% camber. However Fig. 5 shows that the increase in C_L after the stall at
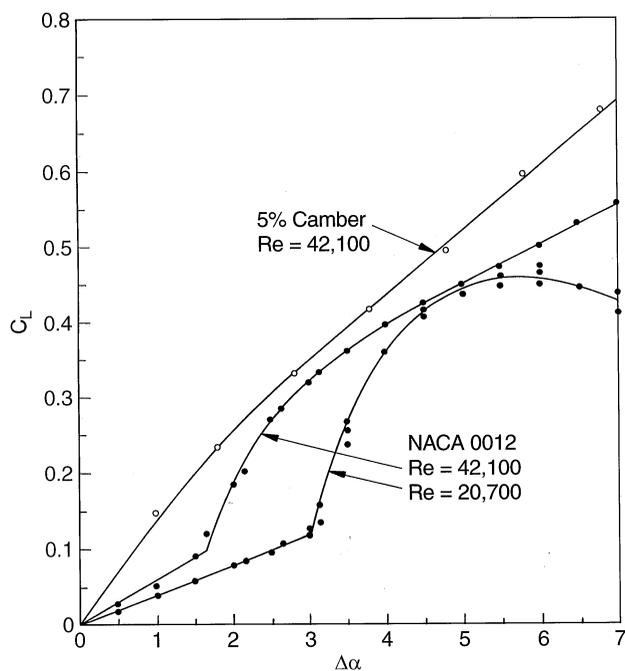
Fig. 3. Effect of increasing Re from 20 700 to 42 100 on the NACA 0012 rectangular planform wing with $A = 6$

Fig. 5. Variation of the lift coefficient (C_L) with the angle of attack from zero lift ($\Delta\alpha$) for aspect ratios $A = 6$ and $A = 4$ rectangular planform wings with the 5% camber profile at $Re = 20\,700$

Fig. 4. Increase of C_L from a small increase in turbulence from 0.02% to 0.10% (with screen) on the NACA 0012 wing ($A = 6$) at $Re = 20\,700$

$\Delta\alpha = 14°$ does not occur when aspect ratio is decreased to four. Schmitz (1941) tested a rectangular planform wing with an aspect ratio of five for a thin (2.9%) plate curved to a 6% camber. His data at Reynolds number equal to 42 000 showed

that C_L did not increase after stall at $C_L = 1.06$. This indicates that the increase in lift after a local stall at $\Delta\alpha = 14°$; as shown in Fig. 5 for the aspect ratio six wing, is a two-dimensional effect that does not occur for aspect ratios of five or less.

As the Reynold number is increased from 20 700 to 42 100 Figs. 2 and 3 show that the initial lift-curve slope of the 5% camber increases 40% from 0.098 to 0.138, which is 26% higher than $(C_L/\alpha) = 2\pi$ for the two-dimensional potential flow lift-curve slope. This indicates that aerodynamic lift at $Re = 42\,100$ is still very different from that at high Reynolds numbers.

Figure 4 shows how much more effective a sharp leading edge is at $Re = 20\,700$. The 0012 with its rounded leading edge had the lowest $(C_L/\alpha)_o$ of only 0.041, while the sharp leading edge of the reversed 0012 had $(C_L/\alpha)_o = 0.064$. Figure 2 shows the thin wedge had $(C_L/\alpha)_o = 0.81$, while the thin plate with 5% camber had $(C_L/\alpha)_o = 0.098$, which is 20% greater than ideal potential flow theory for an aspect ratio six wing with a rectangular planform.

Flow visualization studies were made to help explain the superiority of the sharp leading edge at low Re. Following the procedure of Prandtl and Tietjens (1934) a thin flat plate was hung vertically below the towing carriage moving above a ship model towing tank. The thin (1.5%) plate had a chord of 0.3 m and a span of 1.2 m, its upper tip was above the still water surface, while the lower tip was near the horizontal tank bottom, similar to the procedure described by the Prandtl and Tietjens (1934). With carriage velocities from 0.07 to 0.21 m/s, the Reynolds number range was $20\,900 < Re < 62\,700$. The observations of the movement of the aluminum particles on the free water surface, as the plate moved at constant velocity,

showed that for $Re < 40\,000$ and $\alpha < 8°$, the large leading edge vortex and the large flow separation region on the upper surface were replaced by a continuous shedding of small vortices that rolled along the upper surface so as to greatly decrease the separated flow. The most important observation was that at the trailing edge the velocity on the lower surface was greater than that on the upper surface, and the stagnation point remained at the sharp leading edge for all $\alpha < 8°$. If this proves to be the case for all profiles with sharp leading edges, then the Kutta trailing edge condition is not valid at low Re.

3
Effect of Reynolds number on aerodynamic drag

The decrease of the minimum drag coefficient ($C_{D\min}$) with increasing Reynolds number is shown in Fig. 6 for the NACA 0012 when $C_L = 0$. The straight line approximation is given by $C_D = 0.35\,Re^{-0.25}$, which decreases considerably less than predicted by the Blasius equation $2.66\,Re^{-0.5}$ for the laminar skin friction drag of a zero thickness flat plate, but is slightly more rapid than the decrease given by the turbulent skin friction approximation $C_D = 0.15\,Re^{-0.2}$. These results are all for $C_L = 0 = \alpha$. However Fig. 7 shows that $C_{D\min}$ for the 5% camber occurs at $C_L = 0.34$ at $Re = 20\,700$ when $C_{D\min} = 0.032$, and $C_{D\min} = 0.030$ at $C_L = 0.38$ when $Re = 33\,500$. Fortunately $(C_L/\alpha)_o$ also increases with Re so that $C_{D\min}$ is closely approximated by setting $\Delta\alpha = 3.5°$ at each Re to obtain minimum drag coefficients given in Fig. 6 for the 5% camber. The $C_{D\min}$ values obtained by this procedure were carefully checked at $Re = 20\,700$, $33\,500$, and $42\,100$ by graphing the variation of C_D with C_L to determine that $C_{D\min}$ was approximated within 2% by;

$$C_{D\min} = 0.11\,Re^{-0.125}, \quad 20\,700 \leqslant Re \leqslant 64\,000, \quad 0.34 \leqslant C_L \leqslant 0.44$$

The graph of the variation of C_D with C_L^2 in Fig. 7 shows some agreement with the momentum theory prediction that any finite wing produces an induced drag that varies with C_L^2. For
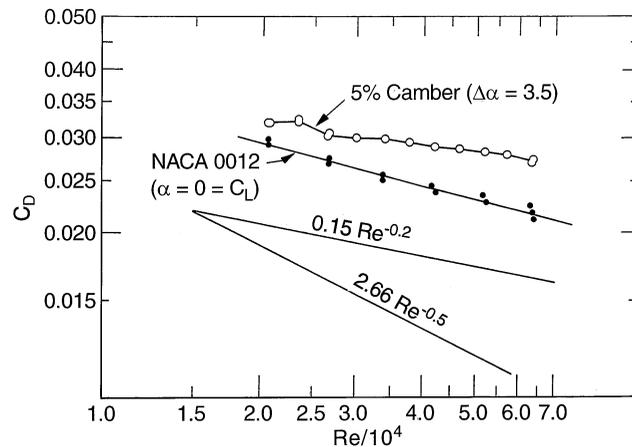
Fig. 6. Variation of minimum C_D *with increasing* Re for the NACA 0012 and the 5% camber rectangular planform wings $A = 6$
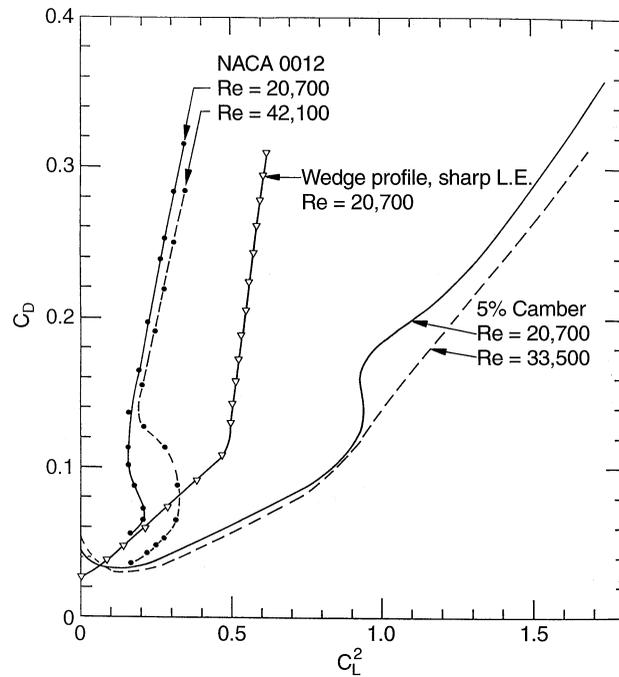
Fig. 7. Variation of the drag coefficient (C_D) with C_L^2 for $A = 6$ rectangular platform wings

example, the 5% camber drag polar can be approximated by the straight line.

$$C_D = C_{De} + K_e C_L^2 = 0.013 + 0.099 C_L^2 \qquad 0.4 < C_L < 0.9$$

$$Re = 20\,700$$

Note that $C_{De} = 0.013 < C_{D\min} = 0.032 < C_{Do} = 0.047$ has no physical significance other than defining the best straight line approximation in Fig. 7. However $K_e = 0.099$ defines the induced drag coefficient $C_{Di} = 0.099 C_L^2$ for the 5% camber, at least for $0.4 < C_L < 0.9$, at $Re = 20\,700$.

Similarly Fig. 7 shows that at $Re = 33\,500$ the straight line approximation to the drag polar for the 5% camber gave the same K_e. This was surprising because a decrease in K_e with Reynolds number was expected because ideal potential flow theory predicts that $K_e \approx (\pi A e)^{-1} = 0.0555$ for an aspect ratio $A = 6$ rectangular planform wing with $e = (1.046)^{-1}$. Unfortunately the C_D data for the 5% camber was unreliable for $C_L > 0.5$ when $Re > 40\,000$.

The approximation to the drag polar for the thin wedge is given by Fig. 7 as

$$C_D = C_{De} + K_e C_L^2 = 0.022 + 0.175 C_L^2, \quad 0 < C_L < 0.7$$

where $C_{De} = 0.022 < C_{D\min} = 0.0263 = C_{Do}$ at $Re = 20\,700$. This shows that K_e is as dependent on the wing profile as it is upon its planform and Reynolds number, since $K_e = 0.175$ for the thin wedge is 77% greater than the corresponding value of $K_e = 0.099$ for the 5% camber at $Re = 20\,700$.

However Fig. 7 shows there is no useful straight line approximation for the drag polar of the NACA 0012 since $K_e \approx 0.18$ only for a very limited range of $0.12 < C_L < 0.45$.

4
Conclusions

The lift force measurements on the NACA 0012 indicate that its sensitivity to variations of the Reynolds number or the turbulence level, make it unsuitable for all $Re < 50\,000$. Applications to wind tunnel models, flow control surfaces and turning vanes would be improved by using thin plates instead of the NACA 0012 profile.

The increase in initial lift-curve slope and the maximum lift coefficient produced by reversing the NACA 0012, so its sharp trailing edge faced the flow, indicates that at $Re = 20\,700$ ideal potential flow is no longer applicable. A sharp leading edge produces more lift than a rounded nose and a sharp trailing edge is no longer necessary for developing lift, so the Kutta trailing edge condition may be irrelevant. The initial lift-curve slopes of the 5% camber are nearly 20% greater than those predicted by potential flow, indicating this theory is not applicable at $Re < 50\,000$. For example, the aspect ratio six wing with 5% camber at $Re = 42\,100$ has $(C_L/\alpha)_o = 0.138$ which is 26% greater than $2\pi/57.3$.

It has also been shown that the induced drag coefficient Ke, which is approximately $1/\pi\,Ae$ at high Reynolds numbers, can be more than doubled at $Re = 20\,700$. Also Ke is shown to be as dependent on the wing's profile as it is upon its planform and Re.

References

Marchman JF (1987) Aerodynamic Testing at Low Reynolds numbers. J Aircraft 24: 107–114

Mueller TJ; Batill SM (1982) Experimental studies of separation on a two-dimensional airfoil at low Reynolds numbers. J Aircraft 20: 457–463

Mueller TJ (1985) Low Reynolds number vehicles. AGARD – graph 288

Prandtl I; Tietjens OJ (1934) Applied hydro- and aeromechanics, pp. 269–271, 296–301, New York: McGraw-Hill

Schmitz FW (1941) Aerodynamics of the model airplane. Redstone arsenal translation, N70-39001, RSIC-721, Nov. 22, 1967